

## 3D super-resolution in fluorescence microscopy imaging

---

**Laure Blanc-Féraud**  
CNRS, UCA, Inria, France

Inverse Problems in microscopy imaging.  
Data Science Artificial Intelligence Master

# Table of contents

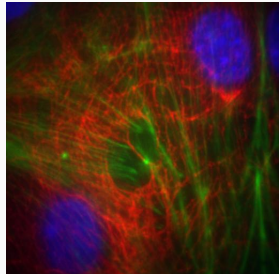
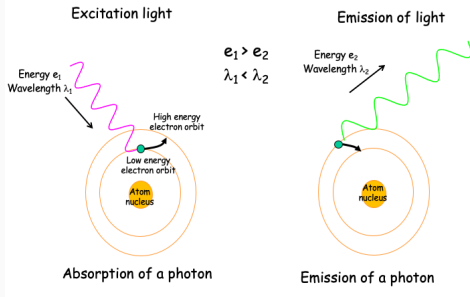


1. Introduction to Fluorescence microscopy
2. Lateral super-resolution
3. 3D super-resolution: COLORME+TIRF-MA
4. Conclusion

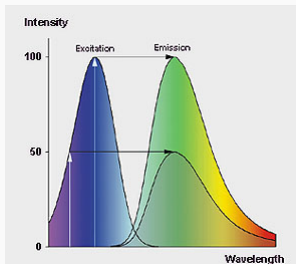
## **Introduction to Fluorescence microscopy**

---

# Fluorescence Microscopy



Fluorescence

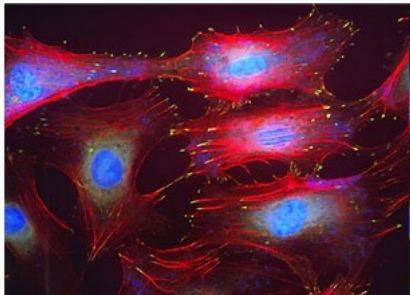


## Fluorescence Microscopy

- ▶ There is **natural fluorescence** in living cells. The first which has been isolated in 1961 was a protein which naturally fluoresces in Green, from the *Aequorea victoria* jellyfish. The protein was named **Green Fluorescent Protein (GFP)**.
- ▶ Its gene can be merged in-vitro to a gene of another protein or structure we want to study. The combining gene is then introduced in cells or embryos and will **synthesis the merging protein** which is then fluorescent. We can see them by microscopy of fluorescence.
- ▶ **living imaging** of cells,...
- ▶ Chemistry Nobel Prize in 2008 to O.Shimomura, M. Chalfie and R. Tsien.

# Fluorescence Microscopy

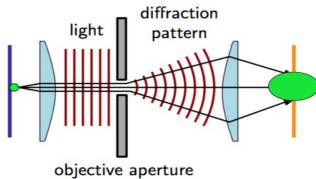
Multiple labeling, with multiple fluorescent markers (GFP, DAPI for nuclei,...)



Example on human hepatic cells with 4 colors. Blue (DAPI): DNA, red (Phalloidin-ALEXA 594): Actin, yellow (ALEXA 488): Vinculin, a membrane adhesion protein), brown (ALEXA 350): von Willebrand factor. Source: <http://www.zeiss.de/>

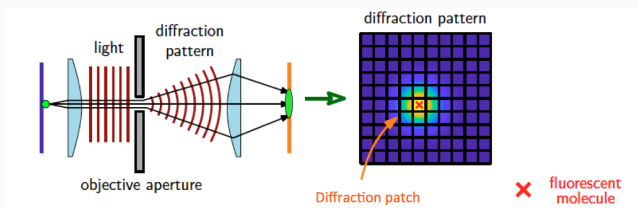
# Optical Imaging

Resolution limited by light diffraction



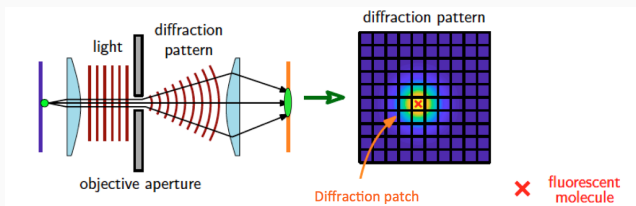
# Optical Imaging

Resolution limited by light diffraction

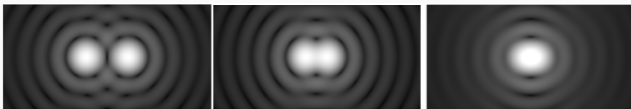


# Optical Imaging

Resolution limited by light diffraction



Example: distinguish between close structures



# Conventional Fluorescent Microscopy Limitations

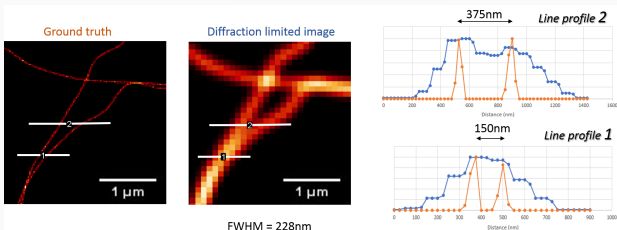
- In image microscopy, spatial resolution is limited by light diffraction phenomena



Point Spread Function (PSF)

- Smallest resolvable distance in the lateral plane (Rayleigh Criterion):

$$d = \frac{0.61\lambda}{NA} \approx 200\text{nm}$$



Resolvable and non-resolvable line profiles

# Conventional Fluorescent Microscopy Limitations

- In image microscopy, spatial resolution is limited by light diffraction phenomena

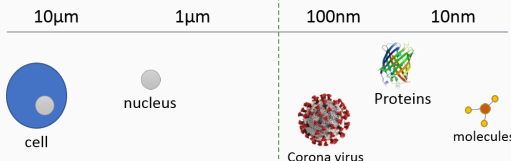


Point Spread Function (PSF)

- Smallest resolvable distance in the lateral plane (Rayleigh Criterion):

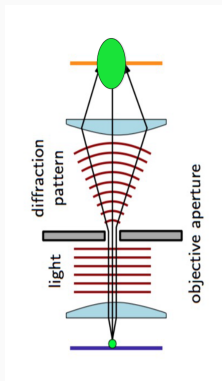
$$d = \frac{0.61\lambda}{NA} \approx 200nm$$

Diffraction limit  
(around 200nm)



Going beyond diffraction limit

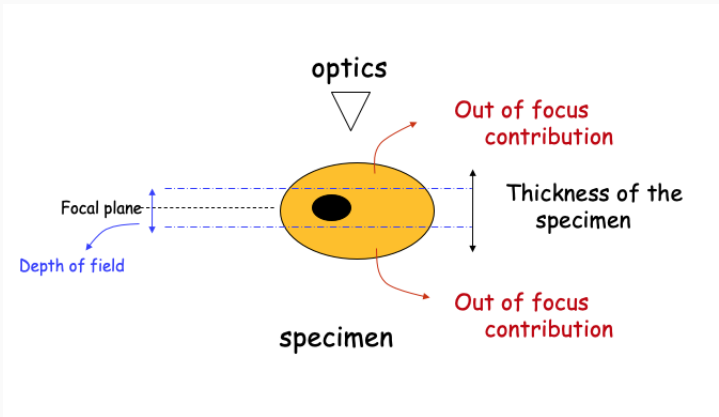
## 3D resolution



- ▶ Lateral plane ( $x,y$ ) limit: 200nm
- ▶ optical axis ( $z$ ) limit: 400nm

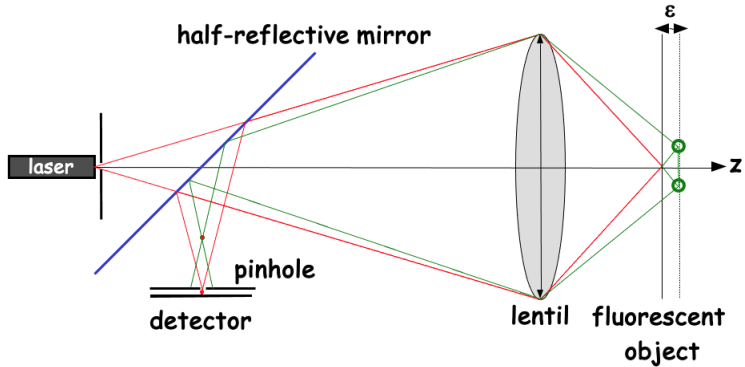


cells are 3D



- ▶ Confocal microscope: use focussed laser, and a pinhole sitting conjugated to the focal plane (i.e. confocal) reject light from out of focus plane.

# Confocal microscope



Best resolution achievable:



## Need for super-resolution

For small structures, **super-resolution** is needed.

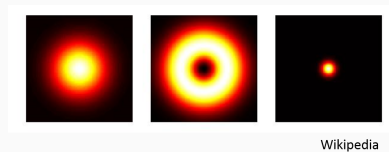
- ▶ With deconvolution we have a gain in resolution
- ▶ Higher resolutions can be achieved with super-resolution methods
- ▶ we will see methods in the lateral plane, then in the radial (optical) axis.

## Lateral super-resolution

---

## State-of-the-art methods for SR microscopy

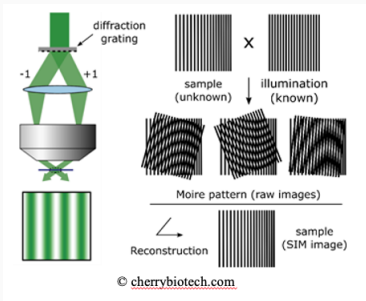
### STimulation-Emission-Depletion [Hell, Wichmann, '94]



- Depletes some of the excited fluorescent molecules, limiting the area of illumination
- Special equipment required, potentially harmful excitation levels

# State-of-the-art methods for SR microscopy

## Structured Illumination Microscopy [Gustafsson & al, '08]



- Special illumination required, limited super-resolution power

## Single Molecule Localization Microscopy

[Betzig, Zhuang, Hess, '06]

- Only few molecules activated for better localisation
- Time consuming acquisition, poor temporal resolution,  
potentially harmful excitation levels

[http://zeiss-campus.magnet.  
fsu.edu/](http://zeiss-campus.magnet.fsu.edu/)

## 2D Super-resolution microscopy: SMLM (continued)

- ▶ activation
- ▶ imaging
- ▶ localization
- ▶ assembling

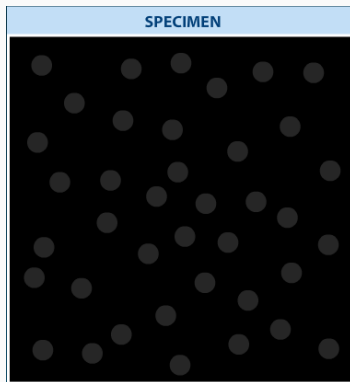


**Figure 1:** PALM microscopy principle. From Zeiss tutorials  
[<http://zeiss-campus.magnet.fsu.edu/tutorials/index.html>]

## 2D Super-resolution microscopy: SMLM (continued)

- ▶ activation
- ▶ imaging
- ▶ localization
- ▶ assembling

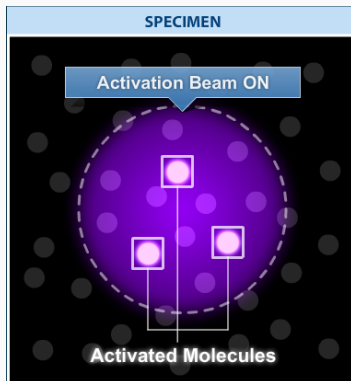


**Figure 1:** PALM microscopy principle. From Zeiss tutorials  
[<http://zeiss-campus.magnet.fsu.edu/tutorials/index.html>]

## 2D Super-resolution microscopy: SMLM (continued)

- ▶ activation
- ▶ imaging
- ▶ localization
- ▶ assembling

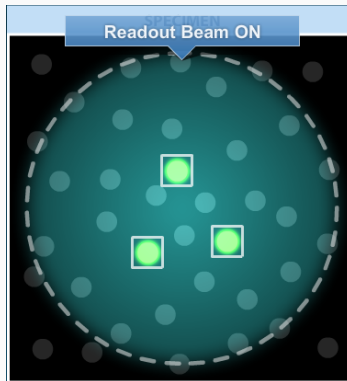


**Figure 1:** PALM microscopy principle. From Zeiss tutorials  
[<http://zeiss-campus.magnet.fsu.edu/tutorials/index.html>]

## 2D Super-resolution microscopy: SMLM (continued)

- ▶ activation
- ▶ imaging
- ▶ localization
- ▶ assembling

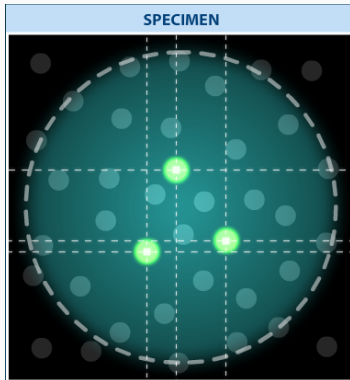


**Figure 1:** PALM microscopy principle. From Zeiss tutorials  
[<http://zeiss-campus.magnet.fsu.edu/tutorials/index.html>]

## 2D Super-resolution microscopy: SMLM (continued)

- ▶ activation
- ▶ imaging
- ▶ localization
- ▶ assembling

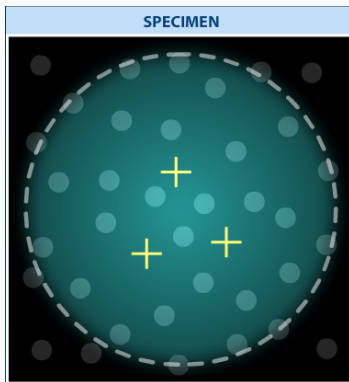


**Figure 1:** PALM microscopy principle. From Zeiss tutorials  
[<http://zeiss-campus.magnet.fsu.edu/tutorials/index.html>]

## 2D Super-resolution microscopy: SMLM (continued)

- ▶ activation
- ▶ imaging
- ▶ localization
- ▶ assembling

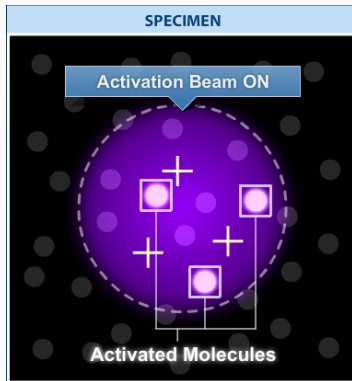


**Figure 1:** PALM microscopy principle. From Zeiss tutorials  
[<http://zeiss-campus.magnet.fsu.edu/tutorials/index.html>]

## 2D Super-resolution microscopy: SMLM (continued)

- ▶ activation
- ▶ imaging
- ▶ localization
- ▶ assembling

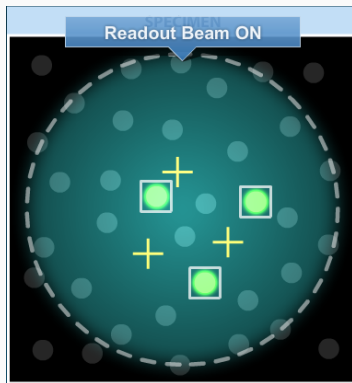


**Figure 1:** PALM microscopy principle. From Zeiss tutorials  
[<http://zeiss-campus.magnet.fsu.edu/tutorials/index.html>]

## 2D Super-resolution microscopy: SMLM (continued)

- ▶ activation
- ▶ imaging
- ▶ localization
- ▶ assembling

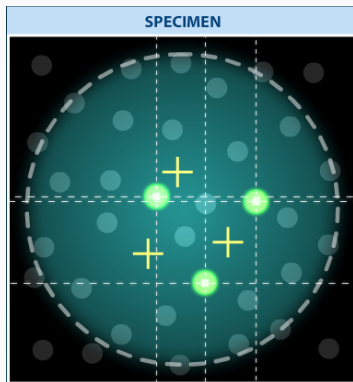


**Figure 1:** PALM microscopy principle. From Zeiss tutorials  
[<http://zeiss-campus.magnet.fsu.edu/tutorials/index.html>]

## 2D Super-resolution microscopy: SMLM (continued)

- ▶ activation
- ▶ imaging
- ▶ localization
- ▶ assembling

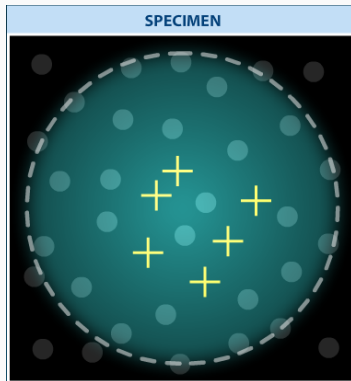
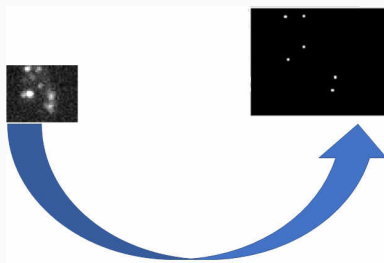
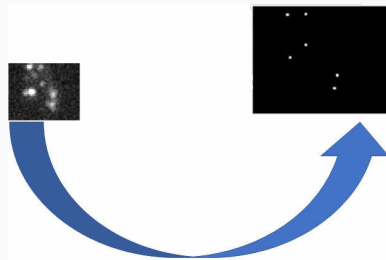


**Figure 1:** PALM microscopy principle. From Zeiss tutorials  
[<http://zeiss-campus.magnet.fsu.edu/tutorials/index.html>]

## 2D Super-resolution microscopy: SMLM (continued)

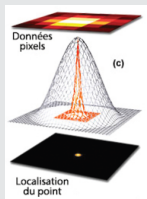


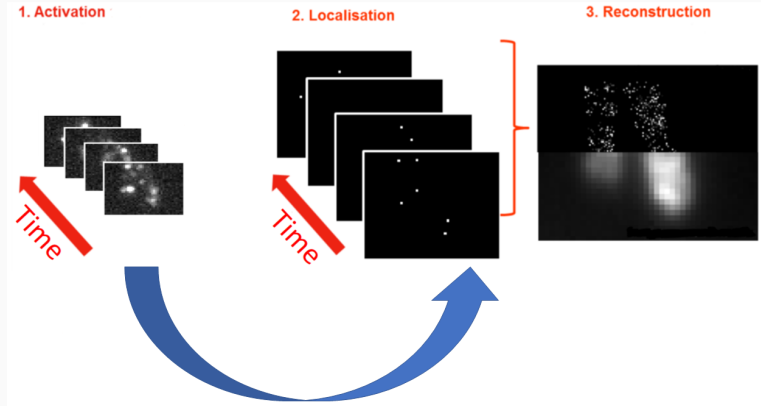
## 2D Super-resolution microscopy: SMLM (continued)



### Localization algorithms

- ▶ Challenge ISBI 2013, 2016 [[Sage'15](#), [Sage'19](#)]
- ▶ PSF fitting, and derived methods for high density molecule localization (e.g. DAOSTORM, [[Holden'11](#)]).
- ▶ Deconvolution and reconstruction on a finer grid (e.g. FALCON, [[Min'14,...](#)])

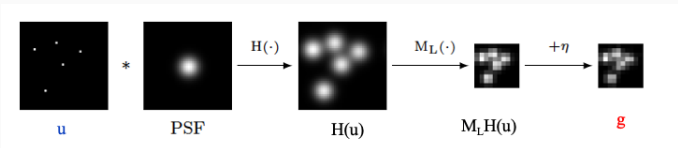




**High density** molecule acquisition to

- ▶ Reduce time and memory
- ▶ Increase temporal resolution (living biological structures)

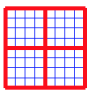
## Decomposition on a finer grid for SMLM



$$\mathbf{g} = M_LH(\mathbf{u}) + \eta$$

$$\mathbf{g} \in \mathbb{R}^m, \quad \mathbf{u} \in \mathbb{R}^n, \quad m \ll n$$

$$A = M_LH$$



$$\min_{\mathbf{u}} \left\{ \frac{1}{2} \|A\mathbf{u} - \mathbf{g}\|_2^2 \right\}$$

- ▶ Ill-posed inverse problem (non unique solution, noise amplification during the inversion)
- ▶ Include sparsity a priori information

# Sparsity

- ▶ A way to include sparsity information on the solution:

$$\min_u \left\{ \frac{1}{2} \|Au - g\|_2^2 + \lambda \|u\|_0 \right\} \text{ where } \|x\|_0 = \#\{x_i, i = 1, \dots, N : x_i \neq 0\}$$

NB:  $\ell_0$ -norm is NOT a norm as  $\|\lambda u\|_0 = \|u\|_0 \neq |\lambda| \|u\|_0$ .

This is **non-continuous, non-convex NP-hard** optimization problem (a *solution cannot be verified in polynomial time w.r.t the dimension of the problem*)

→ see next course on  $\ell_2 - \ell_0$  optimization.

- ▶ A way to deal with sparse optimization is to replace  $\|.\|_0$  by  $\|.\|_1$ ,

$$\min_u \left\{ \frac{1}{2} \|Au - g\|_2^2 + \lambda \|u\|_1 \right\} \text{ where } \|x\|_1 = \sum_{i=1}^N |x_i|$$

This is **continuous, convex, non differentiable** optimization problem.

## $\ell_1$ optimization

Replacing  $\ell_0$ -semi-norm by  $\ell_1$ -norm

$$\hat{x} = \arg \min_{x \in \mathbb{R}^N} \|Ax - d\|_2^2 \text{ subject to } \|x\|_1 \leq K$$

$$\hat{x} = \arg \min_{x \in \mathbb{R}^N} \|Ax - d\|_2^2 + \lambda \|x\|_1$$

with  $\|x\|_1 = \sum_{i=1}^N |x_i|$ .

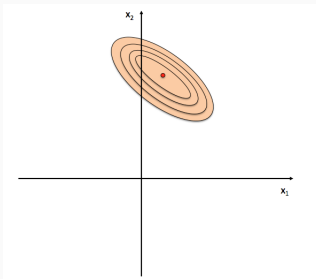
gives easier optimization problems: convex and continuous (but non smooth)

Different (constraint/penalized) formulations are equivalent

$\ell_1$ -norm promotes sparsity

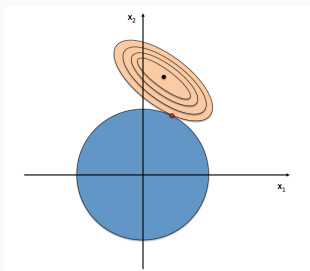
They are known as **Basis Pursuit De-Noising** (BPDN) [Chen et al 98], or **LASSO** [Tibshirani 96] problems.

## $\ell_1$ -norm promotes sparsity



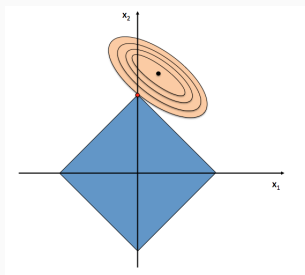
Level lines of  $\|Ax - d\|_2^2$ .

## $\ell_1$ -norm promotes sparsity



Level lines of  $\|Ax - d\|_2^2$  with the  $\ell_2$  constraint  $\|x\|_2 \leq K$ .

## $\ell_1$ -norm promotes sparsity



Level lines of  $\|Ax - d\|_2^2$  with the  $\ell_1$  constraint  $\|\mathbf{x}\|_1 \leq K$ .

## $\ell_1$ -norm promotes sparsity

Let's look at the **penalized** form in the 1-dimensional case: we want to compute

$$\arg \min_{x \in \mathbb{R}} \left\{ g(x) := \frac{1}{2}(x - d)^2 + \lambda|x| \right\}$$

## $\ell_1$ -norm promotes sparsity

Let's look at the **penalized** form in the 1-dimensional case: we want to compute

$$\arg \min_{x \in \mathbb{R}} \left\{ g(x) := \frac{1}{2}(x - d)^2 + \lambda|x| \right\}$$

if  $x \geq 0$  then

$$g(x) = \frac{1}{2}(x - d)^2 + \lambda x$$

The minimum is reached at  $\hat{x} = d - \lambda$ , if  $d \geq \lambda$

if  $d < \lambda$  and  $x \geq 0$  the minimum is reached in  $\hat{x} = 0$

if  $x \leq 0$  then

$$g(x) = \frac{1}{2}(x - d)^2 - \lambda x$$

The minimum is reached at  $\hat{x} = d + \lambda$ , if  $d \leq -\lambda$

if  $d > -\lambda$  and  $x \leq 0$  the minimum is reached in  $\hat{x} = 0$

## $\ell_1$ -norm promotes sparsity

Let's look at the **penalized** form in the 1-dimensional case: we want to compute

$$\arg \min_{x \in \mathbb{R}} \left\{ g(x) := \frac{1}{2}(x - d)^2 + \lambda|x| \right\}$$

if  $x \geq 0$  then

$$g(x) = \frac{1}{2}(x - d)^2 + \lambda x$$

The minimum is reached at  $\hat{x} = d - \lambda$ , if  $d \geq \lambda$

if  $d < \lambda$  and  $x \geq 0$  the minimum is reached in  $\hat{x} = 0$

if  $d \geq \lambda$  then  $\hat{x} = d - \lambda$

and if  $-\lambda \leq d \leq \lambda$  then  $\hat{x} = 0$

if  $x \leq 0$  then

$$g(x) = \frac{1}{2}(x - d)^2 - \lambda x$$

The minimum is reached at  $\hat{x} = d + \lambda$ , if  $d \leq -\lambda$

if  $d > -\lambda$  and  $x \leq 0$  the minimum is reached in  $\hat{x} = 0$

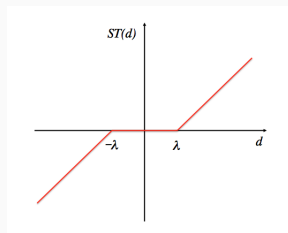
if  $d \leq -\lambda$  then  $\hat{x} = d + \lambda$

The solution is given by the **Soft Threshold** function.

## $\ell_1$ -norm promotes sparsity

The **Soft Threshold** function.

$$\hat{x}(d) = ST_\lambda(d) = \begin{cases} d - \lambda & \text{if } d > \lambda \\ d + \lambda & \text{if } d < -\lambda \\ 0 & \text{if } |d| \leq \lambda \end{cases}$$



## $\ell_1$ -norm promotes sparsity

In the 1-dimensional case, the solution of

$$\arg \min x \in \mathbb{R} \left\{ \frac{1}{2}(d - x)^2 + \lambda|x| \right\}.$$

is reached in

$$\hat{x}(d) = ST_\lambda(d) = \begin{cases} d - \text{sign}(d)\lambda & \text{if } |d| > \lambda \\ 0 & \text{if } |d| \leq \lambda \end{cases} \quad (1)$$

which is the soft-thresholding (ST) function. Then we have that  $\hat{x} = ST_\lambda(d)$  and  $\hat{x} = 0$  for all  $|d| \leq \lambda$ .

**Remark:** if we use the  $\ell_2$ -norm the problem is

$\arg \min x \in \mathbb{R} \left\{ \frac{1}{2}(d - x)^2 + \lambda x^2 \right\}$ . The solution is  $\hat{x} = \frac{d}{1+2\lambda}$  which is different from 0 as soon as  $d \neq 0$ .

## Algorithms for $\ell_2$ - $\ell_1$ optimization

---

- ▶ Convex non smooth optimization
  - ▶ Forward-Backward Splitting (FBS) algorithm for  $\ell_1$ : IST, and Fast version (FISTA,...)
  - ▶ ADMM / Split Bregman Algorithm
  - ▶ ...
-

## Forward-Backward Algorithm (reminder)

The optimization problem is

$$\arg \min_{x \in \mathbb{R}^N} \frac{1}{2} \|Ax - d\|_2^2 + \lambda \|x\|_1$$

But  $\|x\|_1 = \sum_{i=1}^N |x_i|$  is convex but **non differentiable** in all  $x$  ( $x$  such that  $\exists i, x_i = 0$ ).

An algorithm adapted to the minimization of this  $\ell_2 - \ell_1$  non smooth function is the **Forward-Backward Splitting** Algorithm.

Let consider the optimization problem

$$\arg \min_{x \in \mathbb{R}} \{f(x) + g(x)\}$$

where  $f$  is convex, differentiable and  $g$  is continuous, convex, non differentiable but such that its proximal has an explicit form.

**Definition** Proximal of  $g$  :

$$\text{prox}_g(y) = \arg \min_{x \in \mathbb{R}^N} \left\{ \frac{1}{2} \|x - y\|^2 + g(x) \right\}$$

**Example**  $g(\cdot) = \lambda \|\cdot\|_1$ , then

$$\text{prox}_{\|\cdot\|_1}(y) = ST_\lambda(y).$$

# Forward-Backward Algorithm

Optimization problem

$$\arg \min_{x \in \mathbb{R}} \{f(x) + g(x)\}$$

$f : \mathbb{R}^N \rightarrow \mathbb{R}$  convex, differentiable,  $L$ -gradient Lipschitz;

$g : \mathbb{R}^N \rightarrow \mathbb{R}$  continuous, non differentiable, with explicit proximal.

## Forwards-Backward Splitting (FBS) Algorithm

---

**Data:**  $x^0, 0 < \gamma < \frac{1}{L}, TOL$

$k = 0, x^1 = \text{prox}_{\gamma g}(x^0 - \gamma \nabla f(x^0))$

**while**  $(\frac{\|x^{k+1} - x^k\|}{\|x^k\|} > TOL)$  **do**

$x^{k+1} = \text{prox}_{\gamma g}(x^k - \gamma \nabla f(x^k))$

$k = k + 1$

**end**

---

The FBS algorithm converges to a minimizer of  $f + g$  if  $f$  and  $g$  are convex functions [Combettes and Wajs 05], and to a stationary point for non convex functions [Attouch et al 13].

Very easy to use and program on large scale data

### 3.2 Iterative Soft-Thresholding (IST) Algorithm

Penalized form

$$\hat{x} = \arg \min_{x \in \mathbb{R}^N} \frac{1}{2} \|Ax - d\|_2^2 + \lambda \|x\|_1$$

$\frac{1}{2} \|Ax - d\|_2^2$  is  $L$ -gradient Lipschitz ( $L = \|A\|^2$ )

Proximal of  $\|\cdot\|_1$  has explicit expression, this is the Soft Threshold:

$$\text{prox}_{\gamma\lambda\|\cdot\|_1}(y) = ST_{\gamma\lambda}(y)$$

Iterative Soft Thresholding

(IST): Forward-Backward Splitting (FBS) algorithm

$$x^{k+1} = ST_{\gamma\lambda} \left( x^k - \gamma A^t (Ax^k - d) \right)$$

$\gamma < \frac{2}{L}$  is the gradient step.

## Objective

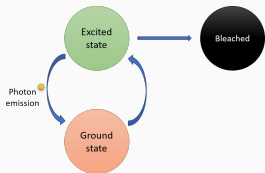
Design an SR model with the following features:

improved temporal resolution

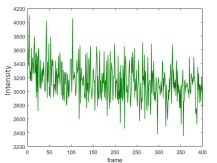
dealing with high density samples

use of standard equipment/conventional fluorophores

# Temporal Fluctuations of molecules



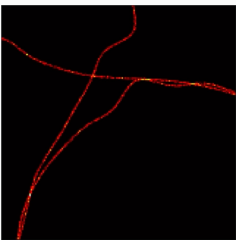
Molecule states



Temporal profile

## Idea

Exploit the temporal **behaviour** and **diversity** of individual molecules.

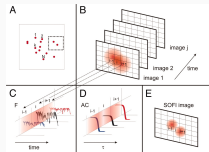


$y_t$ , Low Background, SNR  
≈ 15.6 dB. Video rate: 100  
fps.

$y_t$ . High background, very  
low SNR. Video rate: 100  
fps.

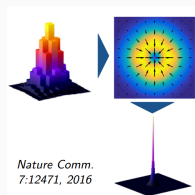
Mean of the molecule  
fluctuations

# Exploiting Stochastic Fluctuations



- Super-Resolution Optical Fluctuation Imaging (**SOFI**)  
[Dertinger & al, '09]

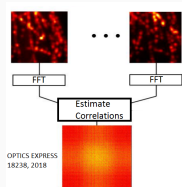
- PSF shrinkage of factor  $\sqrt{n}$  via computation of  $n$ -th order statistics



- Super-Resolution Radial Fluctuations (**SRRF**)

[Gustafsson & al, '16]

- Non-linear transformation of each frame based on radial symmetry computed from local gradients



- SPARity-based SR CORrelation Microscopy (**SPAR-COM**)

[Solomon, Eldar & al, '19]

- exploits  $\ell^1$ -sparsity in the **correlation domain**

# COLORME Method

Two steps

Molecule **localisation** in the Covariance Domain

**Intensity** estimation in the spatial domain

# Mathematical modelling

$\textcolor{red}{Y_t}$

$\textcolor{blue}{U_t}$

## Image formation model

For  $t = 1, \dots, T$ ,  $\textcolor{red}{Y_t} = M_q(H(\textcolor{blue}{U_t})) + \textcolor{black}{N_t} + \textcolor{black}{B}$ ,

$\textcolor{red}{Y_t} \in \mathbb{R}^{N \times N}$ : LR acquisition

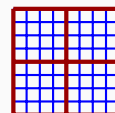
$\textcolor{blue}{U_t} \in \mathbb{R}^{L \times L}$ : HR image ( $L = qN$ )

$M_q \in \mathbb{R}^{N \times L}$ : down-sampling operator

$H \in \mathbb{R}^{N \times N}$ : convolution operator

$\textcolor{black}{N_t}$ : additive white Gaussian noise

$\textcolor{black}{B}$ : stationary background



$$q = 4$$

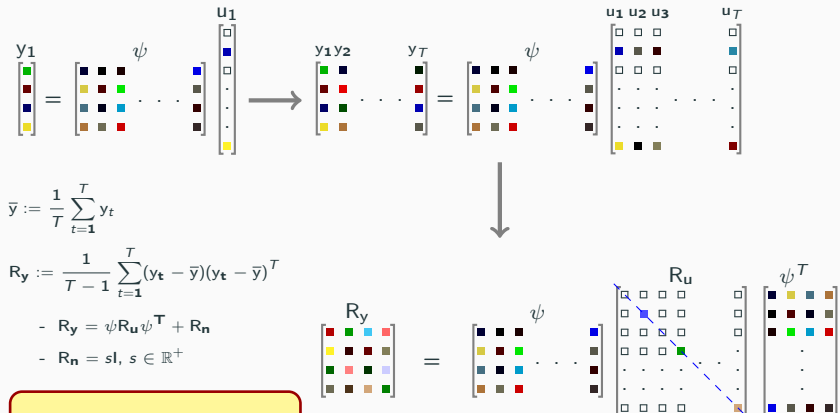
## From Image to Covariance Domain

$$Y_t = M_q(H(U_t)) + N_t + B \xrightarrow{\text{vectorise}} y_t = \psi u_t + n_t + b, \psi \in \mathbb{R}^{M^2 \times L^2}$$



# From Image to Covariance Domain

$$Y_t = M_q(H(U_t)) + N_t + B \xrightarrow{\text{vectorise}} y_t = \psi u_t + n_t + b, \psi \in \mathbb{R}^{M^2 \times L^2}$$



⊗: Column-wise Kronecker product.

## Sparse Regularisation in the Covariance Domain

$$\mathbf{r}_y = (\psi \odot \psi) \mathbf{r}_u + s \mathbf{l}_v \quad (2)$$

$\mathbf{r}_y \in \mathbb{R}^{M^4}$  covariance computed from the observations (blurred and noisy),  
 $\mathbf{r}_u \in \mathbb{R}^{L^2}$  covariance of the true molecules, unknown vector, assumed **sparse** vector,  
 $s \in \mathbb{R}^+$  unknown noise variance.

## Sparse Regularisation in the Covariance Domain

$$\mathbf{r}_y = (\psi \odot \psi) \mathbf{r}_u + s \mathbf{l}_v \quad (2)$$

$\mathbf{r}_y \in \mathbb{R}^{M^4}$  covariance computed from the observations (blurred and noisy),  
 $\mathbf{r}_u \in \mathbb{R}^{L^2}$  covariance of the true molecules, unknown vector, assumed **sparse** vector,  
 $s \in \mathbb{R}^+$  unknown noise variance.

### COLORME: support estimation

$$\arg \min_{\mathbf{r}_u \geq 0, s \geq 0} \frac{1}{2} \|\mathbf{r}_y - (\psi \odot \psi) \mathbf{r}_u - s \mathbf{l}_v\|_2^2 + \lambda R(\mathbf{r}_u),$$

$R(\mathbf{r}_u) = \|\mathbf{r}_u\|_0$ , non continuous, non convex, approximated by  $R = \Phi_{\text{CELO}}$  a continuous exact approximation (still non convex).

$R(\mathbf{r}_u) = \|\mathbf{r}_u\|_1$ , convex, continuous, non differentiable,

$R(\mathbf{r}_u) = TV(\mathbf{r}_u) = \|\nabla(\mathbf{r}_u)\|_1$ , convex continuous, non differentiable.

## Alternate minimisation for support estimation

$R = \Phi_{\text{CELO}}$ ,  $R = \ell^1$  or  $R = \text{TV}$ .

---

COL0RME: Support estimation <sup>1</sup>

---

**Require:**  $\mathbf{r}_u^0 \in \mathbb{R}^{L^2}$ ,  $s^0 \in \mathbb{R}^+$ ,  $\lambda \in \mathbb{R}^+$

**repeat**

$$\mathbf{r}_u^{n+1} = \arg \min_{\mathbf{r}_u \in \mathbb{R}^{L^2}} \frac{1}{2} \|\mathbf{r}_y - (\Psi \odot \Psi) \mathbf{r}_u - s^n \mathbf{l}_v\|_2^2 + \lambda R(\mathbf{r}_u) + \iota_{\geq 0}(\mathbf{r}_u)$$

$$s^{n+1} = \arg \min_{s \in \mathbb{R}} \frac{1}{2} \|\mathbf{r}_y - (\Psi \odot \Psi) \mathbf{r}_u^{n+1} - s \mathbf{l}_v\|_2^2 + \iota_{\geq 0}(s)$$

**until** convergence

---

**Output:**  $\Omega = \{i : (\mathbf{r}_u)_i \neq 0\} = \{i : u_i \neq 0\}$  (support) +  $s$  (noise variance).

## Alternate minimisation for support estimation

$R = \Phi_{\text{CELO}}$ ,  $R = \ell^1$  or  $R = \text{TV}$ .

---

COL0RME: Support estimation <sup>1</sup>

---

**Require:**  $\mathbf{r}_u^0 \in \mathbb{R}^{L^2}$ ,  $s^0 \in \mathbb{R}^+$ ,  $\lambda \in \mathbb{R}^+$

**repeat**

$$\mathbf{r}_u^{n+1} = \arg \min_{\mathbf{r}_u \in \mathbb{R}^{L^2}} \frac{1}{2} \|\mathbf{r}_y - (\Psi \odot \Psi) \mathbf{r}_u - s^n \mathbf{l}_v\|_2^2 + \lambda R(\mathbf{r}_u) + \iota_{\geq 0}(\mathbf{r}_u)$$

$$s^{n+1} = \arg \min_{s \in \mathbb{R}} \frac{1}{2} \|\mathbf{r}_y - (\Psi \odot \Psi) \mathbf{r}_u^{n+1} - s \mathbf{l}_v\|_2^2 + \iota_{\geq 0}(s)$$

**until** convergence

---

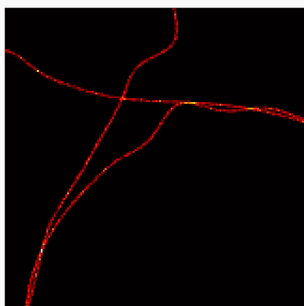
**Output:**  $\Omega = \{i : (\mathbf{r}_u)_i \neq 0\} = \{i : u_i \neq 0\}$  (support) +  $s$  (noise variance).

### Empirical convergence

Convergence is guaranteed if an additional quadratic term is added to the  $s$ -subproblem [Attouch, Bolte, Redont, Soubeiran, '18], but observed in practice.

## Support estimation results: LB/HB datasets

**LB:** low constant background b.



GT. Size: 160x160. Average  
FM/pixel/frame: 10.7.

$y_t$ , SNR  $\approx 15.6$  dB.  $q = 4$ . Video rate:  
100 fps.  $T = 100, \dots, 700$ .

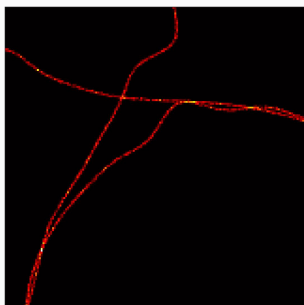
**Spatial pattern:** Microtubules dataset from the SMLM challenge 2016 <sup>1</sup>

**Stochastic temporal profiles:** SOFI simulation tool [Girsault & al, '16].

<sup>1</sup><http://bigwww.epfl.ch/smlm/datasets/index.html>

## Support estimation results: LB/HB datasets

**HB:** high constant background b.



GT. Size: 160x160. Average  
FM/pixel/frame: 10.7.

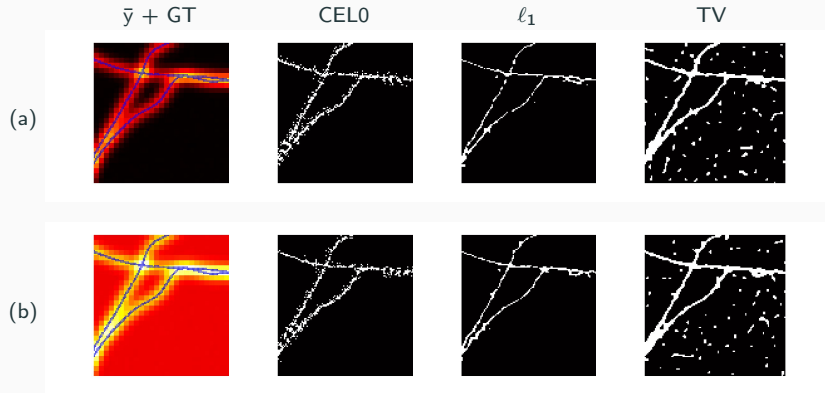
$y_t$ . Very low SNR.  $q = 4$ . Video rate: 100  
fps.  $T = 100, \dots, 700$ .

**Spatial pattern:** Microtubules dataset from the SMLM challenge 2016 <sup>1</sup>

**Stochastic temporal profiles:** SOFI simulation tool ([Girsault & al, '16].

<sup>1</sup><http://bigwww.epfl.ch/smlm/datasets/index.html>

## Support estimation results & comparisons



(a) LB (b) HB  
 $\bar{y}$  & GT (blue) + reconstructions,  $T = 500$ .

Then we can estimate the intensity on the estimated support only.

## Intensity estimation

We have estimated the support  $\Omega$ , and want to estimate the mean intensity.

$$y_t = \psi u_t + n_t + b, \quad t = 1, \dots, T$$

Then on the mean we have

$$\bar{y} = \psi \cdot u + b$$

Estimation only for pixels in  $\Omega \subset \{1, \dots, L^2\}$ .

In the support, assume smoothness of the intensity.

The background must be estimated in the same time.

## Intensity estimation

We have estimated the support  $\Omega$ , and want to estimate the mean intensity.

$$y_t = \psi u_t + n_t + b, \quad t = 1, \dots, T$$

Then on the mean we have

$$\bar{y} = \psi \cdot u + b$$

Estimation only for pixels in  $\Omega \subset \{1, \dots, L^2\}$ .

In the support, assume smoothness of the intensity.

The background must be estimated in the same time.

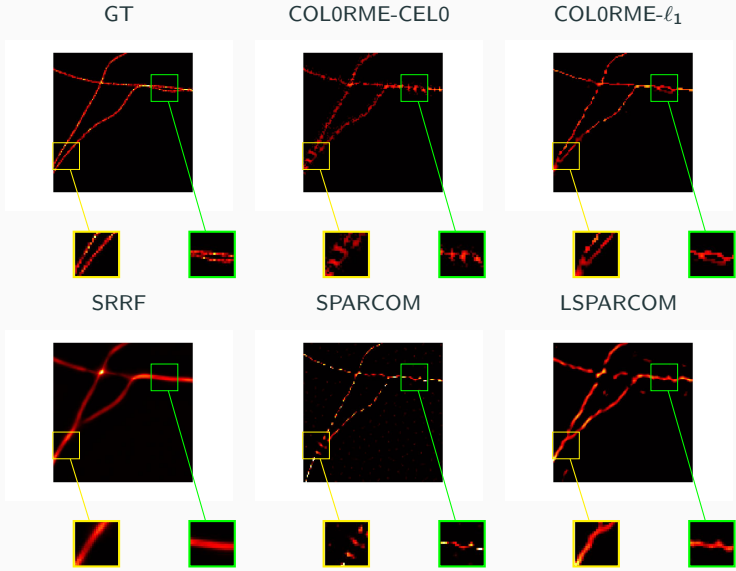
### COL0RME: Intensity estimation

$$\arg \min_{u \in \mathbb{R}^{|\Omega|}, b \in \mathbb{R}^{M^2}} \frac{1}{2} \|\bar{y} - \psi \cdot u - b\|_2^2 + \mu \|\nabla u\|_2^2 + \beta \|\nabla b\|_2^2 + \iota_{\geq 0}(u) + \iota_{\geq 0}(b)$$

where the  $i$ -th column of  $\psi \cdot \in \mathbb{R}^{M^2 \times |\Omega|}$  is extracted from  $\psi$  for all  $i \in \Omega$ .

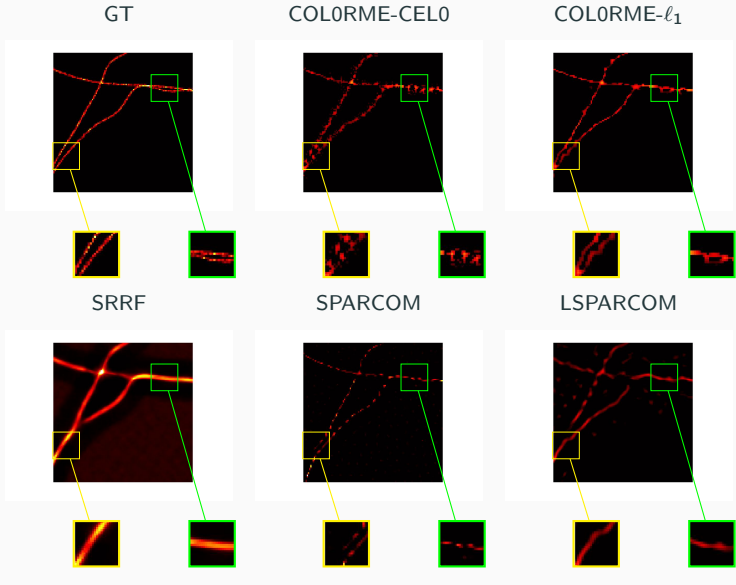
**Algorithm:** relaxation of the constraints + alternate minimisation + gradient/proximal algorithms.

# Intensity estimation on simulated LB, HB data

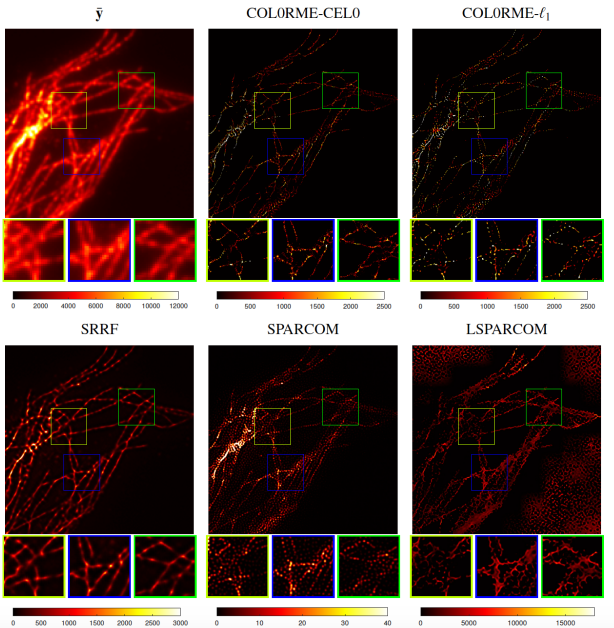


LB,  $T = 500$

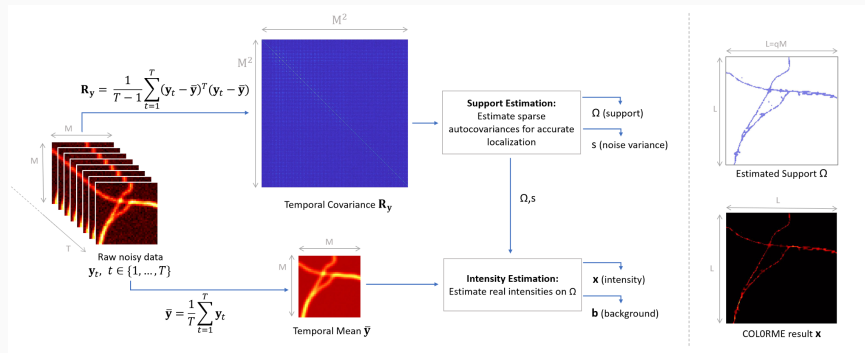
# Intensity estimation on simulated LB, HB data



# Real Data, TIRF acquisition of Tubulin (Alexa fluor 488)



# COLORME summary



## Partial conclusion

**What we have:**

- Lateral super-resolution.



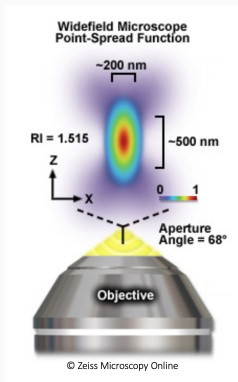
**What is missing:**

- Radial super-resolution.



## 2D to 3D super-resolution

- We have Lateral super-resolution.



Point Spread Function of a  
Widefield microscope: resolution  
is worse in the axial direction.

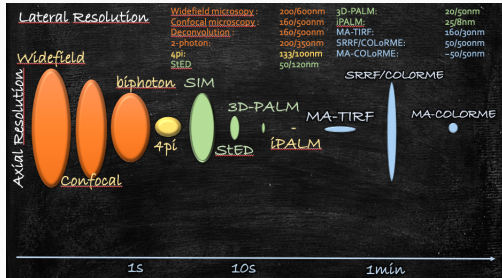


- We need Axial super-resolution
- 3D super-resolution

# Axial/3D Fluorescence Microscopy Super-resolution

- ▶ Confocal [Pawley, '06], lightsheet microscopes [Keller & al, '08]
- ▶ 3D SMLM (Helicoidal PSF [Sage & al, '19], interferometry iPALM [Shtengel & al, '09]),
- ▶ STED: STimulation-Emission-Depletion [Hell, Wichmann, '94],
- ▶ 3D SIM: Structured Illumination Microscopy [Gustafsson & al, '08]
- ▶ 4pi microscope [Cremer & Cremer, '71, Bewersdorf & al, '04]
- ▶ MA-TIRF Multi-Angle Total Internal Reflection Fluorescence Microscope  
super-resolution at the interface [Olveczky & al, '97] [Yang & al, '10] [Boulanger & al  
14] [Fan & al, '19]

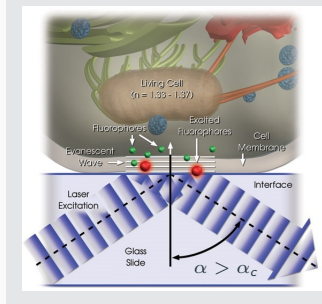
# Axial/3D Fluorescence Microscopy Super-resolution



- ▶ MA-TIRF Fluorescence Microscope
  - super-resolution **at the interface**
  - not harmful** for the biological sample

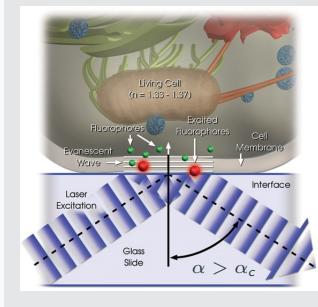
# TIRF microscopy

## Total Internal Reflection Fluorescence (TIRF) [Axelrod, '08]



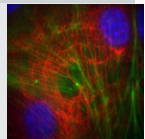
# TIRF microscopy

## Total Internal Reflection Fluorescence (TIRF) [Axelrod, '08]

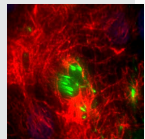


**Limit** the observed region to a **thin layer** (100nm to 1 $\mu$ m),  
**Remove** out-of-focus signal,  
**Ideal** to observe sub-cellular structures.

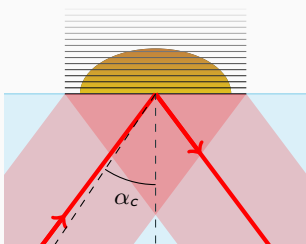
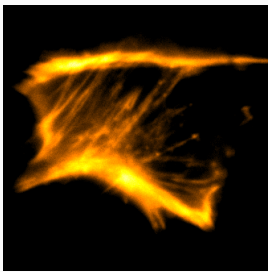
Widefield



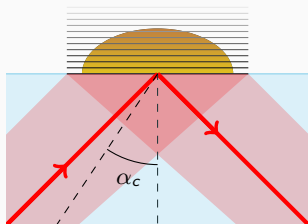
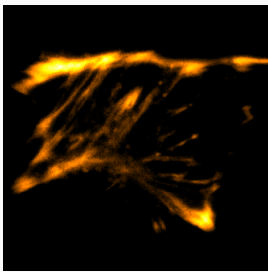
TIRF



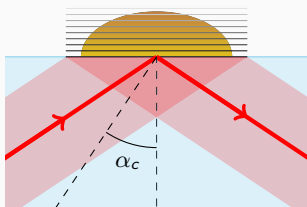
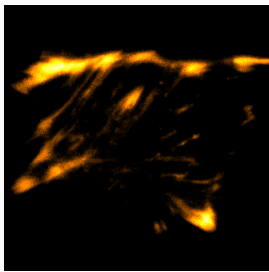
## From Single TIRF to Multi-Angle TIRF



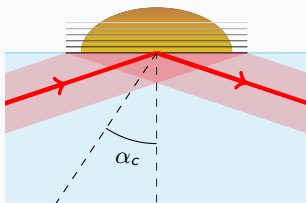
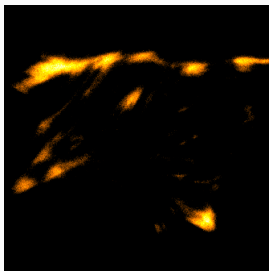
## From Single TIRF to Multi-Angle TIRF



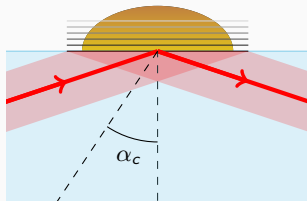
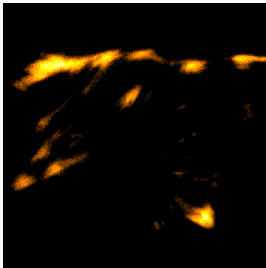
## From Single TIRF to Multi-Angle TIRF



## From Single TIRF to Multi-Angle TIRF



# From Single TIRF to Multi-Angle TIRF



Access to **3D information**,  
Potential for **axial super-resolution**,  
**Reconstruction algorithms** are needed.

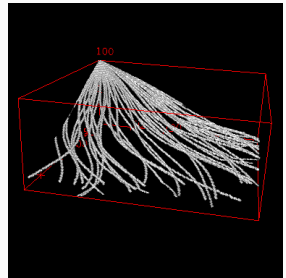
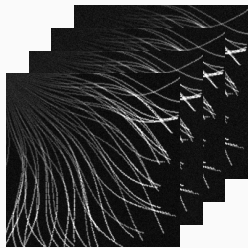
~200nm



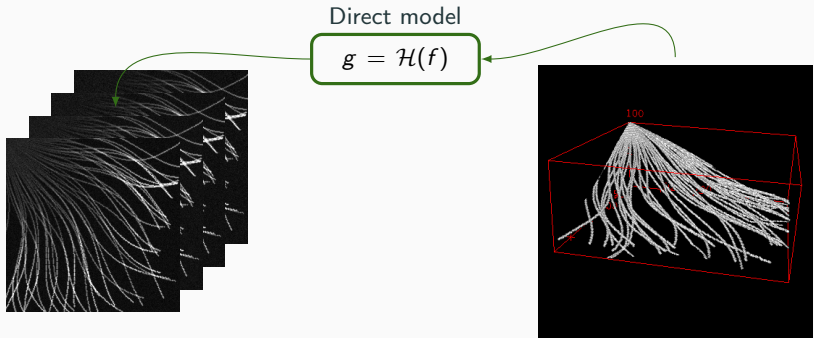
~400nm



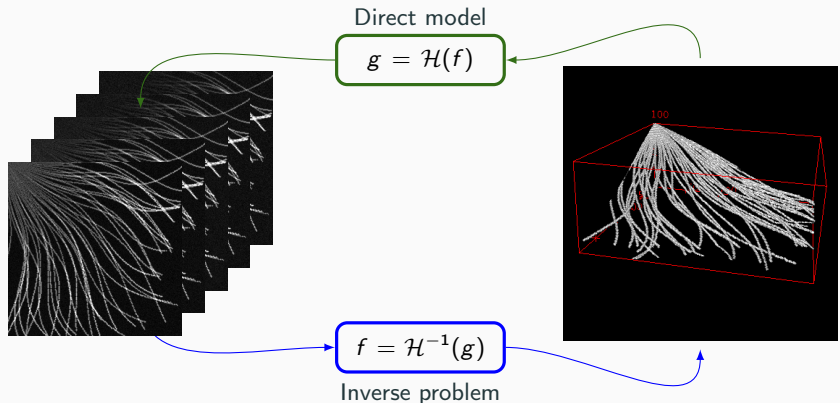
## From single TIRF to Multiple-Angle TIRF - *Reconstruction*



## From single TIRF to Multiple-Angle TIRF - *Reconstruction*



## From single TIRF to Multiple-Angle TIRF - *Reconstruction*



## Related Works

Methods based on **shape prior**:

- membranes [Reichert & Truskey, '92] [Burmeister & al, '94] [Olveczky & al, '97] [Saffarian & Kirchhausen 08] [Stabley & al, '15] [Dos Santos & al, '16]
- vesicles (3D particles) [Rohrbach, '00] [Loerke al, '02] [Soubies & al, '14]
- microtubules (curvilinear structures) [Yang, '10][Jin & al, '17]

Direct 3D volume acquisition (successive acquisitions and photobleaching)  
[Fu & al, '16]

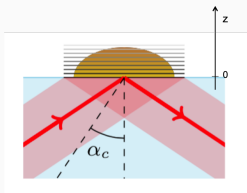
**Regularized variational approaches** [Boulanger & al 14] [Zheng & al, '18] [Fan & al, '19]

## From single TIRF to Multiple-Angle TIRF - Reconstruction Model

The illumination by evanescent wave has exponential decay:  
 $I_0 \cdot \exp(-zp(\alpha))$  where

$I_0$  : intensity of the evanescent field at  
the interface (i.e.  $z = 0$ )

$p(\alpha) = \frac{4\pi n_i}{\lambda_{\text{exc}}} (\sin^2(\alpha) - \sin^2(\alpha_c))$ : in-  
verse of the penetration depth of the  
evanescent wave

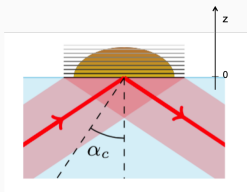


## From single TIRF to Multiple-Angle TIRF - Reconstruction Model

The illumination by evanescent wave has exponential decay:  
 $I_0 \cdot \exp(-zp(\alpha))$  where

$I_0$  : intensity of the evanescent field at  
the interface (i.e.  $z = 0$ )

$p(\alpha) = \frac{4\pi n_i}{\lambda_{\text{exc}}} (\sin^2(\alpha) - \sin^2(\alpha_c))$ : in-  
verse of the penetration depth of the  
evanescent wave



Then the observation for a given pixel  $x_m$  and for a given angle  $\alpha$  is

$$g(x_m, \alpha) = I_0(\alpha) \int_0^{z_{\max}} \exp(-zp(\alpha)) \cdot f(x_m, z) dz + b_{x_m}$$

## From single TIRF to Multiple-Angle TIRF - *Reconstruction Model*

Discrete model:

$$\mathbf{g}_q = \mathbf{T}_q \mathbf{f} + \mathbf{b},$$

$\mathbf{f} \in \mathbb{R}_{\geq 0}^N \rightarrow$  3D discrete **fluorophores density**,

$\mathbf{T}_q \in \mathbb{R}^{M \times N} \rightarrow$  Discrete **TIRF operator** associated to the incident angle  $\alpha_q$ ,

$\mathbf{g}_q \in \mathbb{R}^M, q = 1,.., Q \rightarrow$  **TIRF images** acquired with the incident angles  $\{\alpha_q > \alpha_c\}$ ,

$\mathbf{b} \in \mathbb{R}^M \rightarrow$  **Background** signal.

Variational formulation of the inverse problem Find  $(\hat{\mathbf{f}}, \hat{\mathbf{b}})$  solution of

$$\arg \min_{\substack{\mathbf{f} \in \mathbb{R}^N \\ \mathbf{b} \in \mathbb{R}^M}} \left( \sum_{q=1}^Q \frac{1}{2} \|T_q \mathbf{f} + \mathbf{b} - \mathbf{g}_q\|_2^2 + \mu_0 \|\nabla \mathbf{b}\|_2^2 + \mu_1 \|\nabla \mathbf{f}\|_1 + \mu_2 i_{\geq 0}(\mathbf{f}) \right).$$

## Joint reconstruction and background estimation

Variational formulation of the inverse problem Find  $(\hat{\mathbf{f}}, \hat{\mathbf{b}})$  solution of

$$\arg \min_{\substack{\mathbf{f} \in \mathbb{R}^N \\ \mathbf{b} \in \mathbb{R}^M}} \left( \sum_{q=1}^Q \frac{1}{2} \|T_q \mathbf{f} + \mathbf{b} - \mathbf{g}_q\|_2^2 + \mu_0 \|\nabla \mathbf{b}\|_2^2 + \mu_1 \|\nabla \mathbf{f}\|_1 + \mu_2 i_{\geq 0}(\mathbf{f}) \right).$$

Augmented problem Find  $(\hat{\mathbf{f}}, \hat{\mathbf{b}}, \hat{\mathbf{v}}_1, \hat{\mathbf{v}}_2)$  in

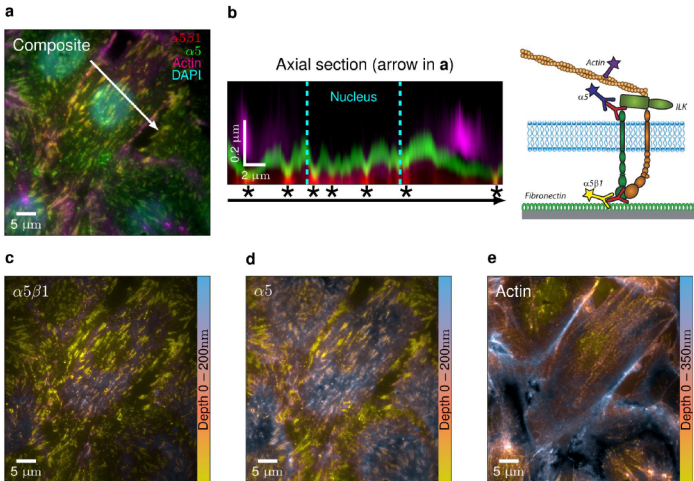
$$\arg \min_{\substack{\mathbf{f}, \mathbf{b} \\ \{\mathbf{u}_i\}_{i=0}^2}} \left( \sum_{q=1}^Q \frac{1}{2} \|T_q \mathbf{f} + \mathbf{b} - \mathbf{g}_q\|_2^2 + \mu_0 \|\nabla \mathbf{b}\|_2^2 + \mu_1 \|\mathbf{v}_1\|_1 + \mu_2 i_{\geq 0}(\mathbf{v}_2) \right)$$

such that  $\mathbf{v}_1 = \nabla \mathbf{f}$ ,  $\mathbf{v}_2 = \mathbf{f}$ .

Simultaneous-Direction Method of Multipliers (SDMM) algorithm

[Combettes & Pesquet, '11, Gabay & Mercier, '76]

## 6) Experiments - Study of Fibronectin Assembly Units



**3D super-resolution:**  
**COLORME+TIRF-MA**

---

# 3D super-resolution

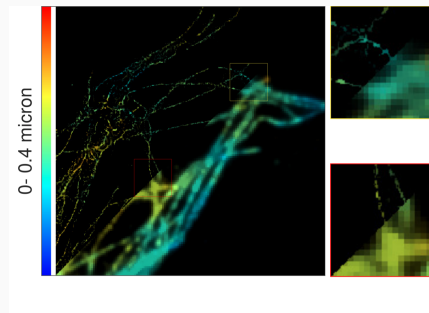
## COLORME + TIRF-MA

Tubulin filaments of endothelial cells marked with Alexa Fluor 488,

Acquisition of sequence of 500 images at each angles (4 angles only),

Reconstruction at each angle with COLORME, background removed, intensity estimated: lateral super-resolution,

Reconstruction of the radial information with TIRF-MA.



MA-TIRF reconstruction on the mean of the stack and on COL0RME images

## Conclusion

---

# Conclusion

## Super-resolution in Fluorescence Microscopy

### COLORME

- ▶ Formulation of the SR problem in the **covariance domain** to exploit temporal independence of **standard fluorescent emitters**,
- ▶ "Colouring step" computing **image intensities** ≠ SOFI, SPARCOM (sparse covariance images  $r_u$ ), SRRF (radiality maps)
- ▶ Applicability to large variety of biological observations
- ▶ Last course: how to improve by using GAN

### MA-TIRF

- ▶ is a method of choice for the observation of **subcellular** processes,
- ▶ System achieves **20-30nm** of resolution from **100 up to 400 nm**.

### COLORME +TIRF-MA reconstruction

- ▶ 3D super-resolution method at the interface, complementary to 3D SIM / 3D STED / 3D SMLM / iPALM

## References i

-  Hedy Attouch, Jérôme Bolte, and Benar Fux Svaiter, *Convergence of descent methods for semi-algebraic and tame problems: proximal algorithms, forward-backward splitting, and regularized Gauss-Seidel methods*, Mathematical Programming, 137 (2013), pp. 91–129.
-  Scott Shaobing Chen, David L Donoho, and Michael A Saunders, *Atomic decomposition by Basis Pursuit*, SIAM journal on scientific computing, 20 (1998), pp. 33–61.
-  Patrick Combettes and V. Wajs, *Signal recovery by proximal forward-backward splitting*, Multiscale Modeling and Simulation, 4(4), (2005), pp. 1168-1200.
-  R. Tibshirani, *Regression shrinkage and selection via the lasso*, Journal of the Royal Statistical Society, 46 (1996), pp. 431–439.